

One-neutron transfer in Ni-Ni interactions below the barrier

J. Wiggins, R. Brooks, M. Beckerman, S. B. Gazes,* L. Grodzins, A. P. Smith, S. G. Steadman, and Y. Xiao
Laboratory for Nuclear Science, Massachusetts Institute of Technology, Cambridge, Massachusetts 02139

F. Videbaek

The Niels Bohr Institute, University of Copenhagen, Copenhagen, Denmark

(Received 9 January 1985)

Using γ -ray photopeak intensities, excitation functions of one-neutron transfer to excited states in reaction products have been measured from about 20% and 15% below the fusion barrier to above barrier energies for $^{58}\text{Ni} + ^{64}\text{Ni}$ and $^{64}\text{Ni} + ^{64}\text{Ni}$ reactions, respectively. For $^{58}\text{Ni} + ^{64}\text{Ni}$, the one-neutron transfer cross section is greater than 1 mb at 20% below the barrier. The results are well described by distorted-wave Born approximation calculations using spectroscopic factors deduced from light-ion transfer measurements.

I. INTRODUCTION

As early as 1952, it was realized that the study of sub-Coulomb nuclear reactions between heavy ions should result in essentially model independent nuclear structure information. In an analogy to the sub-Coulomb (d,p) "Oppenheimer-Phillips process,"¹ Breit, Hull, and Gluckstern² suggested that sub-Coulomb nucleon transfer reactions should be progressively less sensitive to the ion-ion interaction with decreasing bombarding energy. Although many sub-Coulomb measurements of (d,p) and (p,d) reactions (as well as lighter heavy-ion pickup and stripping reactions) have been employed in the study of nucleon densities at large radial distances in heavy nuclei, until now there have been no measurements at sub-Coulomb energies of transfer cross sections for reactions where both target and projectile are heavy ($A > 30$).

This paper presents the first measurements of one-nucleon transfer cross sections at sub-Coulomb energies between symmetric, heavy ions. One-nucleon transfer cross sections extending from $\approx 20\%$ below to 4% above the phenomenological fusion barrier have been deduced from four-point singles γ -ray angular distributions. These characteristic γ rays identify nucleon transfer leading to particular excited states of a transfer product. The results show that the simple one-step one-nucleon transfer model, as embodied in the distorted-wave Born approximation (DWBA), can describe the one-nucleon transfer cross sections at bombarding energies less than 5% below the barrier. For a well matched reaction, one-neutron transfer at 20% below the barrier can be as large as 1 mb to just a single state of one of the transfer products. The total one-neutron transfer cross section is estimated to be about 20–50% larger than this.

Previously, our group at MIT has measured sub-barrier fusion cross sections³ for $^{64,58}\text{Ni} + ^{64,58}\text{Ni}$. Simple barrier-penetration models that provide satisfactory descriptions of fusion cross sections from above-barrier bombardments cannot reproduce the below-barrier fusion excitation functions.⁴ When normalized by the appropriate geometric cross sections, the sub-barrier fusion excitation

functions, with respect to the barrier height, of $^{64}\text{Ni} + ^{64}\text{Ni}$ and $^{58}\text{Ni} + ^{58}\text{Ni}$ are nearly identical, while that of $^{58}\text{Ni} + ^{64}\text{Ni}$ is significantly larger.³ From Q -value systematics it has been argued⁵ that this isotopic dependence of sub-barrier fusion is consistent with nucleon, and especially nucleon pair, transfers enhancing the probability of fusion. If the Q value for transfer is positive or if the barrier of the resulting system is lower, additional kinetic energy would then be available to effectively lower the barrier to fusion.^{1,5} Coupled channels calculations,⁶ however, indicate that inelastic scattering can also increase the cross section for sub-barrier fusion.

The one-neutron reaction from $^{58}\text{Ni} + ^{64}\text{Ni}$ has a slightly negative Q value (-0.66 MeV) and is well Q matched. Transfer reactions from identical projectile-target combinations ($^{64}\text{Ni} + ^{64}\text{Ni}$ and $^{58}\text{Ni} + ^{58}\text{Ni}$) have significantly more negative Q values and are not well Q matched. The sub-barrier one-neutron transfer cross section from $^{58}\text{Ni} + ^{64}\text{Ni}$ is about 8 times larger than that of $^{64}\text{Ni} + ^{64}\text{Ni}$, when comparison is made with respect to the fusion barrier for each reaction. At the barrier, fusion cross sections for both target-projectile combinations are about equal and the cross section for one-neutron transfer for the well Q matched $^{58}\text{Ni} + ^{64}\text{Ni}$ is at least twice that of fusion, but one-neutron transfer from $^{64}\text{Ni} + ^{64}\text{Ni}$ has about half the cross section of fusion. At 5 MeV below the fusion barrier, the one-neutron transfer cross section from each projectile-target combination is at least a factor of 50 larger than the corresponding fusion cross section. Even without considering nucleon pair transfer, one-neutron transfer cross sections are large enough that only a relatively small fraction could couple to fusion and explain this isotopic dependence of sub-barrier fusion.

II. EXPERIMENTAL METHOD

A. Apparatus and technique

The experiment was performed at the Brookhaven National Laboratory Tandem Van de Graaff Facility using ^{58}Ni and ^{64}Ni beams of 2–6 particle nanoampere (pnA)

intensity, pulsed in a 10 sec cycle consisting of 7.5 sec beam-on and 2.5 sec beam-off intervals. The beam spot was focused at low intensity to less than 2 mm diam on a ZnS scintillator and was centered through 1.9 cm diam and 1.6 cm diam tantalum apertures placed, respectively, 14 cm and ≈ 1 m upstream to absorb any beam halo. The $200 \mu\text{g}/\text{cm}^2$ thick targets were isotopically enriched ^{58}Ni (99.93%) and ^{64}Ni (96.48%).

The characteristic γ rays were detected with Ge detectors at laboratory angles of 40° , 78° , 144° , and 147° . For $^{58}\text{Ni} + ^{64}\text{Ni}$, a detector was placed at 100° instead of 40° . Solid angles subtended by the γ -ray detectors were in the range of 140–190 msr. A separate run measuring only 155 MeV $^{58}\text{Ni} + ^{64}\text{Ni}$ was limited to just 0.3 pA beam intensity on a $560 \mu\text{g}/\text{cm}^2$ thick ^{64}Ni target and employed anti-Compton shielding of a 90° Ge(Li) detector. For all runs, silicon surface barrier detectors were placed at 44.5° and 46° . Particle and γ -ray singles data, along with scaler information, were sorted into four separate time gates: one during beam-on and three of equal duration within the 2.5 sec beam-off interval. Subtractions of spectra were performed to remove room background and long-lived activities.

The spectra from both the silicon detector beam monitors and the γ -ray detectors show that about $10 \mu\text{g}/\text{cm}^2$ of ^{12}C and ^{16}O were on the upstream surface of the targets. These impurities resulted in part from the target manufacture and in part from buildup during the run.

Absolute cross sections were determined from an average of two normalizations. One used the observed yields from Coulomb excitation of the target and projectile at each of the measured γ -ray angles. When this normalization procedure included the calculated γ -ray angular distributions,⁷ agreement between γ -ray detectors was typically better than 5%. The other normalization was determined by using the measured elastic scattering peaks at 44.5° and 46.0° . The elastic data were normalized to the Rutherford cross section at lower energies. At the highest energy they were normalized to the elastic scattering data calculated in the optical model using the potential of Christensen *et al.*⁸ The Coulomb-excitation and elastic-scattering normalization procedures agree to 10%, except they disagree by 15% at $E_{\text{c.m.}} < 80$ MeV for the $^{58}\text{Ni} + ^{64}\text{Ni}$ reaction. Uncertainty in absolute normalization is estimated to be 15%. The $^{64}\text{Ni} + ^{64}\text{Ni}$ results have an additional 5% uncertainty because the precise scattering angle and beam spot geometry were not known. This additional uncertainty results from calculations indicating that the small number of Mott oscillations across the acceptance angles of the particle detectors do not necessarily average to reproduce the Rutherford scattering cross sections used for normalization.

It is apparent from the sample spectra in Fig. 1 that broad full-energy peaks and Compton continua from Coulomb excitation dominate the spectra. The evaporation residues from Ni-Ni interactions recoil within a narrow forward cone at about half-beam velocity, and can be identified by the velocity-characteristic energy shift of relatively narrow full-energy peaks between the forward and backward directions. In the investigation of possible contaminating peaks, these Doppler shifts were employed to

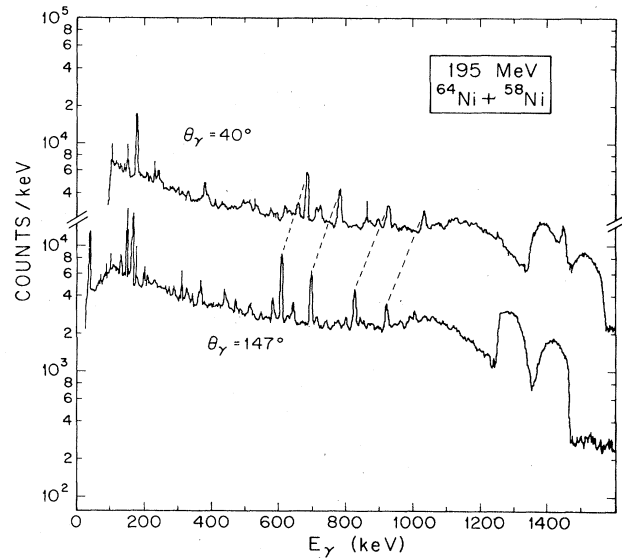


FIG. 1. Measured, room background corrected, γ -ray spectra for $E_\gamma < 1600$ keV, from 195 MeV $^{64}\text{Ni} + ^{58}\text{Ni}$. The upper spectrum is measured at $\vartheta_\gamma = 40^\circ$, the lower is from $\vartheta_\gamma = 147^\circ$. The pair of broad full-energy peaks on the right result from Coulomb excitation of the projectile and target. Details of the shapes of these peaks result from the product angular distributions. The diagonal lines connect forward and backward angle full-energy peaks having positions and Doppler shifts characteristic of evaporation residues from projectile fusion with carbon or oxygen contaminants. Most peaks exhibiting smaller shifts result from evaporation residues from fusion with the ^{58}Ni target.

identify γ rays from evaporation residues resulting from projectile fusion with the nickel target and with the ^{16}O and ^{12}C contaminants.

Sub-barrier nucleon transfer has a rather broad angular distribution peaked in the back direction. This provides a kinematic signature for transfer-characteristic γ rays. Ignoring symmetry, following a head-on collision the projectilelike transfer product is nearly at rest in the laboratory and the targetlike partner recoils in the forward direction at near beam velocity. Transfer characteristic photopeaks from the targetlike partner are Doppler shifted to higher (or lower) energy if measured at a forward (or back) angle. Peaks become skewed following the kinetic energy sharing between transfer products as the sub-barrier transfer angular distribution extends appreciably out from 180° . The kinematic signature for transfer shown in the angle dependent shapes of photopeaks is distinct from that resulting from compound nucleus evaporation residues, room background, Coulomb excitation, and other beam-related γ -ray activities. In this way, the photopeaks can be unambiguously associated with characteristic γ decay following nucleon transfer to specific excited states of distinct reaction products.

For example, Fig. 2(a) displays the measured γ -ray spectra from 195 MeV $^{64}\text{Ni} + ^{58}\text{Ni}$ in the region of the 155.5 keV γ ray, characteristic of population of the $\frac{3}{2}^-$

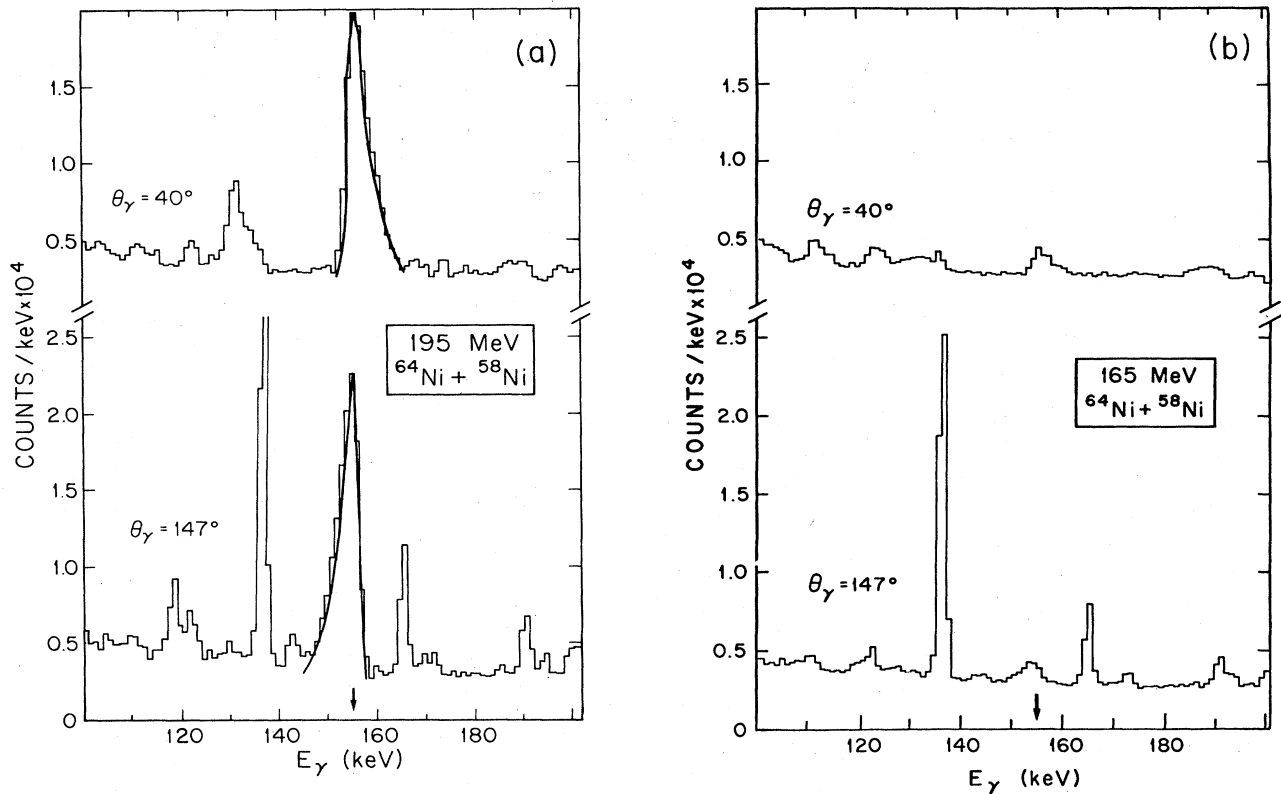


FIG. 2. (a) Measured, room background corrected, γ -ray spectra at 40° (top) and 147° (bottom) in the region of the transfer-characteristic 155.5 keV ^{63}Ni γ -ray transition resulting from 195 MeV $^{64}\text{Ni} + ^{58}\text{Ni}$. The arrow indicates 155.5 keV. Since the ^{63}Ni transfer product is nearly at rest in the laboratory, the maximum of the peak is near 155 keV. The high energy tail from 40° and low energy tail from 147° result from the angular distribution extending forward of 180° for this one-neutron transfer reaction. The bold smooth curve is the predicted peak shape using the product angular distribution calculated in the DWBA, the detector solid angles of 144 msr and 195 msr, and a 2 keV energy resolution. Sharp peaks in just the 147° spectrum result from Coulomb excitation of a nearby tantalum beam collimating slit. (b) Measured, room background corrected, γ -ray spectra at 40° (top) and 147° (bottom) in the region of the transfer-characteristic 155.5 keV ^{63}Ni γ -ray transition resulting from 165 MeV $^{64}\text{Ni} + ^{58}\text{Ni}$. The arrow indicates 155.5 keV. The spectra are to be compared with those in (a), where the cross section for population of the 155.5 keV state is about 30 times larger.

excited state of ^{63}Ni . Comparison of these transfer-characteristic peaks with those from Coulomb excitation appearing near 1300 keV in Fig. 1 shows that peak shapes from Coulomb excitation and nucleon transfer are distinct. The angular distribution of transfer products calculated in the DWBA are used to predict peak shapes. Figure 2(a) shows that the measured peak shapes are consistent with the calculated angular distribution. Discussion of these DWBA calculations follows in Sec. IV A.

The photopeak shapes are characteristic of the single neutron transfer at all measured bombarding energies. Figure 2(b) displays the corresponding γ -ray spectra from one of the lowest bombarding energies, 165 MeV $^{64}\text{Ni} + ^{58}\text{Ni}$. The spectra from the high and low energy bombardments are presented on approximately the same vertical scale. Although the transfer cross section from

the 165 MeV bombardment is $\approx 3\%$ of that from 195 MeV, the 155.5 keV γ -ray peak from the lower bombarding energy still exhibits the skewed high energy tail when measured from the forward angle, and the characteristic low energy tail is observed from the backward angle. These peak shapes are also consistent with the γ -ray peak shapes predicted from angular distributions calculated in the DWBA. Furthermore, the corresponding photopeaks from the inverse reaction of $^{58}\text{Ni} + ^{64}\text{Ni}$, where the roles of fast and slow recoil products are exchanged, show the expected Doppler shifts and inverted shapes, and the cross sections for both projectile-target combinations are in agreement. In the bombardments studied, every full-energy peak observed to exhibit these shape characteristics has been identified to be associated with one-nucleon transfer. The photopeak, therefore, is correctly identified.

B. Limitations of the technique

The lack of data for sub-Coulomb nucleon transfer between heavy, nearly symmetric nuclei is due primarily to the difficulty of detecting the transfer products. Total nucleon transfer cross sections to excited states can be measured employing the detection of characteristic γ rays, but the technique has limitations. First, nucleon transfer to the ground states of both transfer products cannot be measured. In the case of odd- A nickel isotopes from ^{57}Ni to ^{65}Ni , the lowest excited states are $\frac{1}{2}^-$, $\frac{3}{2}^-$, and $\frac{5}{2}^-$. These are described as almost pure shell-model neutron states.⁹ The states are below 500 keV excitation for $A > 58$ and the ordering changes with increasing mass of the nickel isotopes. So, for one-neutron transfer reactions to these odd- A products, ground state population would not be expected to be particularly favored or disfavored. The DWBA calculations support this expectation.

Second, since just the characteristic γ rays are used to identify the reaction, nucleon transfer populating states at higher excitation of the detected transfer product may γ decay through the lower-lying characteristic gating transition. The measured γ -ray intensity would then contain contributions from transfer leading to states at higher excitation in this product nucleus, making a spectroscopic study difficult. The highest excited state of the $\frac{1}{2}^-$, $\frac{3}{2}^-$, $\frac{5}{2}^-$ triplet decays predominantly directly to the ground state. Because of Q -value matching for transfer and the large fraction of one-particle strength concentrated in this triplet, feeding from higher excited states would be expected to constitute a relatively small fraction of the measured transfer cross sections at sub-barrier energies. DWBA calculations support this as well.

Finally, unlike direct particle measurement, particular final state pairs of transfer products cannot be selected in this singles γ -ray measurement. The transfer identified by a gating transition from a transfer product corresponds to a sum over connecting final states of the other final nucleus. This makes a spectroscopic study of individual states even more difficult, but allows a measure of the total amount of transfer leading to the gating transition. It will be shown that only a few of the low-lying excited states of each product nucleus need be considered for the reactions presented. In this particular experiment, cross sections for transfer characteristic γ rays with $E_\gamma > 300$ keV are difficult to measure in the presence of the rather large Compton continuum, but this is not a serious problem for the transitions presented.

III. EXPERIMENTAL RESULTS

Sub-barrier one-neutron transfer cross sections are presented for three beam-target combinations. Observed transfer characteristic γ rays include those from the 86.9 keV ($\frac{5}{2}^-$) and 155.5 keV ($\frac{3}{2}^-$) states in ^{63}Ni following $^{64}\text{Ni} + ^{64}\text{Ni}$, $^{64}\text{Ni} + ^{58}\text{Ni}$, and $^{58}\text{Ni} + ^{64}\text{Ni}$ reactions. That these γ rays are associated with transfer is established by (a) agreement between the $^{64}\text{Ni} + ^{58}\text{Ni}$ and $^{58}\text{Ni} + ^{64}\text{Ni}$ bombardments; (b) the fact that the ^{63}Ni -characteristic peaks from the latter reaction are Doppler shifted (target-like) but those from $^{64}\text{Ni} + ^{58}\text{Ni}$ are near the transition energy (projectilelike); and (c) observed Doppler-broadened

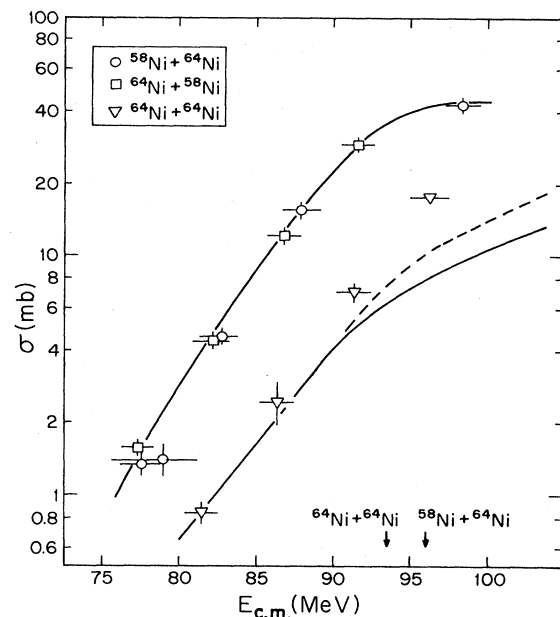


FIG. 3. Measured excitation functions for population of the 155.5 keV $\frac{3}{2}^-$ state of ^{63}Ni from $^{58}\text{Ni} + ^{64}\text{Ni}$ pickup (circles), $^{64}\text{Ni} + ^{58}\text{Ni}$ stripping (squares), and $^{64}\text{Ni} + ^{64}\text{Ni}$ pickup and stripping (triangles). The solid curves result from DWBA calculations using the optical potential from Ref. 8, and the dashed curve from that of Ref. 14. Horizontal bars through data show the variation of projectile energy within the target; the vertical lines represent statistical error. Arrows near the bottom indicate the positions of phenomenological fusion barriers.

peak shapes that are characteristic of transfer.

Figure 3 shows measured excitation functions for population of the 155 keV $\frac{3}{2}^-$ state of ^{63}Ni . Cross sections extracted from different γ -ray detectors are observed to vary less than 20%, so angular distributions are nearly isotropic. The total cross sections are then determined from an unweighted average using angles where photopeaks of interest are relatively free of contaminating background lines. The horizontal bar on data points depicts the variation of projectile energy within the 200 $\mu\text{g}/\text{cm}^2$ targets. An effective bombarding energy is calculated from the slope of the excitation function, and the cross section at this energy reproduces the measured cross section when an integration is performed over the target thickness. The data point from $^{58}\text{Ni} + ^{64}\text{Ni}$ at $E_{\text{c.m.}} = 78.9$ MeV was taken from the previously mentioned low beam intensity bombardment using a 560 $\mu\text{g}/\text{cm}^2$ thick target.

The photopeak resulting from population of the $\frac{3}{2}^-$ state of ^{63}Ni from ^{64}Ni (^{64}Ni , ^{63}Ni) ^{65}Ni consists of two components, one near the transition energy and another, Doppler shifted, originating from the decay of the faster recoil partner. The 155.5 keV cross sections for $^{64}\text{Ni} + ^{64}\text{Ni}$ include both the stripping and pickup components.

The measured intensities of the 86.9 keV γ rays suffer from angle dependent and bombarding energy dependent

normalization factors, principally due to the exceptionally long lifetime (1.7 μ sec) of this state. Fast forward-going (at 0°) ^{63}Ni recoils which are excited to this $\frac{5}{2}^-$ state would decay in the beam stop, far from the γ -ray detectors. The observed strength is due to the recoils that stop in the target or in the wall of the 2.5 cm diam glass scattering chamber. We have estimated the magnitude of this effect using the geometry of the experimental setup and the calculated transfer product angular distributions, performed in the DWBA (see Sec. IV A). For the $^{58}\text{Ni} + ^{64}\text{Ni}$ bombardments, the measured intensities from 40° are predicted to be above the values resulting from the assumption that γ -ray decay occurred at the target by about 25% and 50% from the high and low energy bombardments, respectively. The measured intensities from 147° are expected to be underpredicted by about 20% and 35%, respectively. The effect is smaller from the ^{64}Ni bombardment of a ^{58}Ni target, because many of the slow, forward-moving ^{63}Ni recoil nuclei stop in the target.

Data of Fig. 4 for population of this 86.9 keV state of ^{63}Ni result from an unweighted average of the measured intensities from each angle, and are expected to be within 25% of the correct values. This measured excitation function shown in the upper portion of Fig. 4 still has the same basic shape as that of the 155.5 keV transition, with an intensity of about 20% of the $^{58}\text{Ni} + ^{64}\text{Ni}$ and $^{64}\text{Ni} + ^{58}\text{Ni}$ $\frac{3}{2}^-$ populations and about $\frac{1}{3}$ of that of the 155.5 keV state from the corresponding $^{64}\text{Ni} + ^{64}\text{Ni}$ reactions.

For $^{64}\text{Ni} + ^{58}\text{Ni}$ and $^{58}\text{Ni} + ^{64}\text{Ni}$ reactions, full-energy peaks that would correspond to one-neutron transfer populating the 339.4 keV ($\frac{5}{2}^-$) and 465 keV ($\frac{3}{2}^-$) states of ^{59}Ni are observed. The measured excitation function for population of the $\frac{5}{2}^-$ state of ^{59}Ni at 339.4 keV shown in the lower part of Fig. 4 has the same shape and about 30% of the cross section of the $\frac{3}{2}^-$ state shown in Fig. 3. Although a peak is observed at the expected positions, the 465 keV data cannot be reliably separated from the background.

IV. DISCUSSION

A. DWBA predictions

Calculations of Coulomb excitation demonstrate that for $E_{c.m.} < 90$ MeV, the target and projectile are both in their ground states at the distance of closest approach with at least a 90% probability. Sub-barrier one-neutron transfer calculations are performed in the DWBA using the computer codes¹⁰ ONEFF and DIWRI, modified to include symmetry for the $^{64}\text{Ni} + ^{64}\text{Ni}$ calculations. The same distorted-waves potential that was used to determine the data normalization is also employed in the calculation of nucleon transfer cross sections. This Woods-Saxon potential⁸ has the following parameters: $V = -40$ MeV, $W = -25$ MeV, $r = 1.248$ fm, $a = 0.65$ fm, $r_c = 1.32$ fm. This potential is chosen because it agrees with global systematics.¹¹ No significant differences between calculations are observed below $E(\text{lab}) = 180$ MeV for a variety of similar potentials. Making the distorting potential weaker does not effect the calculated sub-barrier transfer cross

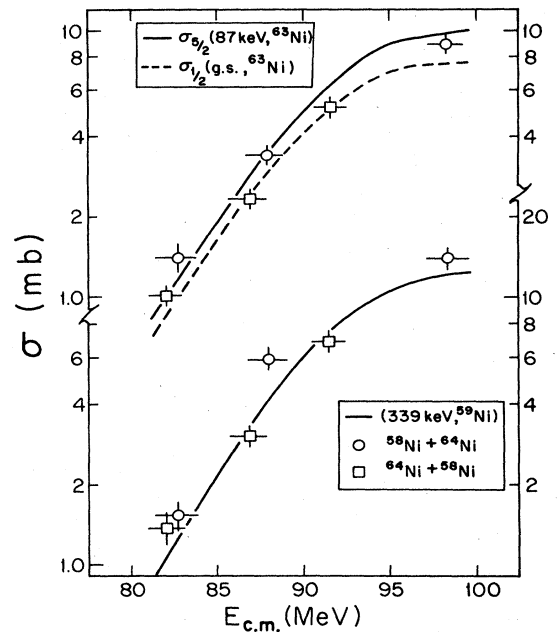


FIG. 4. The upper part of the figure shows measured excitation functions for populations of the 86.9 keV $\frac{5}{2}^-$ state of ^{63}Ni following $^{58}\text{Ni} + ^{64}\text{Ni}$ pickup (circles) and $^{64}\text{Ni} + ^{58}\text{Ni}$ stripping (squares) reactions. These 86.9 keV data suffer from bombarding energy (and projectile-target) dependent normalization factors estimated to be in the range of 0.75 to 1.25, as explained in Sec. III. The solid curve shows a DWBA calculation of direct population of this 86.9 keV state. The dashed curve is from the same calculation for the population of the $\frac{1}{2}^-$ ground state of ^{63}Ni . The lower part of the figure shows the corresponding measured excitation functions for population of the 339.4 keV $\frac{5}{2}^-$ state of ^{59}Ni , and the solid curve shows the DWBA calculation for direct population of this state.

sections, but, in the limit of using an unreasonably deep and wide potential of $V = -80$ MeV, $W = -50$ MeV, $r = 1.49$ fm, $a = 0.64$ fm, $r_c = 1.25$ fm, the 160 MeV sub-barrier transfer is reduced by 40%. Calculations performed in the post and prior formalisms agree to 5%.

Calculations are sensitive to the nucleon binding potential used because the magnitudes of the bound state wave functions near the distance of approach are modified. Changing the bound state radius parameter from $r = 1.20$ to 1.25 fm has the effect of increasing the calculated transfer cross sections by about 40%. The neutron wave functions are calculated in a Woods-Saxon well with parameters $r = 1.25$ fm, $a = 0.65$ fm, and a well depth that reproduces the measured binding energy. A Thomas-type spin-orbit interaction of strength $\lambda = 25$ is included.

The calculated cross section for, e.g.,

$$^{64}\text{Ni}(^{58}\text{Ni}, ^{59}\text{Ni})^{63}\text{Ni}(155 \text{ keV}),$$

is obtained assuming that the 155 keV $\frac{3}{2}^-$ state in ^{63}Ni is not populated from above,

$$\sigma_{3/2}(^{63}\text{Ni}) = S_{3/2}(\text{d,t}) \sum_{ij} \sigma_j^{\text{DW}}(E_i^*) S'_{ij}(\text{d,p}). \quad (1)$$

The sum over j encompasses $\frac{1}{2}^-$, $\frac{3}{2}^-$, $\frac{5}{2}^-$, $\frac{7}{2}^-$, and $\frac{9}{2}^+$ states of ^{59}Ni , and i identifies the appropriate excitation energies E_i^* . The (d,p) spectroscopic factors

$$S'_{ij}[^{58}\text{Ni}(\text{d,p})^{59}\text{Ni}(E_i^*)]$$

used in the present calculations are taken from low energy and Coulomb stripping reactions¹² and are listed in Table I. The spectroscopic strength of the 155 keV state of ^{63}Ni is described by $S_{3/2} = 4S'_{3/2} = 2.42$ from $^{64}\text{Ni}(\text{d,t})^{63}\text{Ni}$ pickup reactions¹³ at the higher bombarding energy of 15 MeV.

The calculation for $^{64}\text{Ni}(^{64}\text{Ni}, ^{63}\text{Ni})^{65}\text{Ni}$ is performed in the same manner. Absolute spectroscopic factors used for ^{65}Ni are listed in Table I. These are an average of the measured values¹² from light-ion low-energy and Coulomb one-neutron pickup reactions. In performing this average, it is important to use spectroscopic factors deduced from analyses using nearly the same bound state parameters.

The upper solid curve in Fig. 3 represents this DWBA calculation for $^{58}\text{Ni} + ^{64}\text{Ni}$ using the assumptions given above. Since the calculations are relatively insensitive to the distorting ion-ion potential below the barrier, and since the bound state parameters are fixed, this leaves no adjustable parameters in the calculation. The close agreement of calculation with data gives confidence in using the DWBA model calculations for sub-barrier one-neutron transfer reactions between heavy ions in this mass region. Furthermore, the calculated angular distribution is generally correct because the shapes of the photopeaks are predicted, e.g., Fig. 2.

The lower solid curve in Fig. 3 shows the corresponding calculation for one-neutron pickup and stripping from $^{64}\text{Ni} + ^{64}\text{Ni}$. The dashed line is from the same calculation using the potential from Bond *et al.*¹⁴ These calculations underpredict the transfer cross sections near and above

TABLE I. Spectroscopic factors to ^{59}Ni and ^{65}Ni .

^{59}Ni j^π	E^* (keV)	$S'(\text{d,p})$	^{65}Ni j^π	E^* (keV)	$S'(\text{d,p})$
$\frac{1}{2}^-$	465	0.52	$\frac{1}{2}^-$	65	0.62
				1270	0.02
$\frac{3}{2}^-$	0	0.59		1416	0.08
	878	0.10		2139	0.06
	1735	0.01	$\frac{3}{2}^-$	309	0.03
$\frac{5}{2}^-$	339	0.71		689	0.14
	1680	0.18	$\frac{5}{2}^-$	0	0.27
	1953	0.02			
	2635	0.07	$\frac{9}{2}^+$	1013	0.56
$\frac{7}{2}^-$	1948	0.04			
$\frac{9}{2}^+$	3061	0.55			

the barrier, but agree with the data at below barrier bombardments.

Calculations of transfer leading to direct population of the ground state and the 86.9 keV state of ^{63}Ni are performed using the spectroscopic factors listed in the fourth column of Table II. Even with the energy dependent normalization problem discussed in Sec. III, the latter calculation provides an excellent fit of the $^{64}\text{Ni}(^{58}\text{Ni}, ^{59}\text{Ni})^{63}\text{Ni}$ data presented in the upper portion of Fig. 4. These calculations estimate the sum of one-neutron transfer to the lowest $\frac{1}{2}^-$, $\frac{3}{2}^-$, and $\frac{5}{2}^-$ states of ^{63}Ni to be about 1.33 times that of the 155.5 keV ($\frac{3}{2}^-$) state. Using measured spectroscopic factors for transfer to higher excited states,¹³ along with estimates of the probability of these states decaying through the 155.5 keV ($\frac{3}{2}^-$) state of ^{63}Ni , total one-neutron transfer cross sections from sub-barrier $^{58}\text{Ni} + ^{64}\text{Ni}$ and $^{64}\text{Ni} + ^{64}\text{Ni}$ are predicted to be in the range of 1.2–1.5 times those shown in Fig. 3 for population of just the 155.5 keV state.

The calculated population of the 339.4 keV ($\frac{5}{2}^-$) state of ^{59}Ni from $^{64}\text{Ni}(^{58}\text{Ni}, ^{59}\text{Ni})^{63}\text{Ni}$ is determined from a sum over ^{63}Ni final states with spectroscopic factors listed in Table II. The spectroscopic factor to this $\frac{5}{2}^-$ state at 339.4 keV of ^{59}Ni is taken from the (d,p) stripping reaction:¹² $S_{5/2} = (2j+1)S'_{5/2} = 0.72$. The agreement of calculation with data in the lower portion of Fig. 4 shows again that sub-barrier one-nucleon transfer cross sections between heavy ions can be successfully calculated in the simple DWBA. The fifth column of Table II, which lists the cross sections of populating higher excited states of ^{63}Ni , supports the earlier proposition that transfer to higher excited states constitutes a relatively small fraction of the $^{63}\text{Ni}(155.5 \text{ keV})$ cross section. The largest contribution is from neutron transfer populating the $\frac{3}{2}^-$ state of ^{63}Ni at 517.5 keV, which has measured decay branches to all three states at lower excitation. The branch to the 155.5 keV state is about¹⁵ 85%.

Using calculated nucleon pair spectroscopic amplitudes,¹⁶ it is predicted from DWBA calculations that neutron pair transfer cross sections are dominated by ground state transfers. Although it is well known¹⁷ that the DWBA often significantly underpredicts nucleon pair transfer, the calculated pair transfer cross section is less

TABLE II. Spectroscopic factors to ^{63}Ni . The fifth column shows calculated one-neutron transfer cross sections from 180 MeV $^{64}\text{Ni} + ^{58}\text{Ni}$ leading to states in ^{63}Ni leaving ^{59}Ni in the $\frac{5}{2}^-$ state at 339.4 keV excitation.

^{63}Ni j^π	E^* (keV)	$S'(\text{d,t})$	$(2j+1)S'$	$\sigma_{5/2}(^{59}\text{Ni}, 339.4 \text{ keV})$ (mb)
$\frac{1}{2}^-$	0	0.24	0.47	0.093
	1000.9	0.26	0.52	0.095
$\frac{3}{2}^-$	155.5	0.61	2.42	1.631
	517.5	0.21	0.82	0.446
$\frac{5}{2}^-$	86.9	0.57	3.43	0.051
$\frac{7}{2}^-$	1787	0.03	0.23	0.025
	1899	0.06	0.45	0.048
$\frac{9}{2}^+$	1294	0.08	0.82	0.084

than a fourth of that for one-neutron transfer. Of course, the γ -ray technique cannot be used to measure nucleon pair transfer leading to the ground states of both products, but the importance of this reaction channel should not be overlooked.

B. Connection with sub-barrier fusion

If one-nucleon transfer is associated with the larger sub-barrier fusion cross sections³ for $^{58}\text{Ni} + ^{64}\text{Ni}$ as compared to those of $^{58}\text{Ni} + ^{58}\text{Ni}$ and $^{64}\text{Ni} + ^{64}\text{Ni}$, then $^{58}\text{Ni} + ^{64}\text{Ni}$ sub-barrier reactions would be expected to exhibit more transfer. This is the case, even considering just the one-neutron transfer leading to the $\frac{3}{2}^-$ state at 155.5 keV excitation in ^{63}Ni . These fusion excitation functions just above the barrier can be described by calculating transmission coefficients using inverted harmonic oscillator potentials³ with the parameters listed in Table III. In showing transfer and fusion cross sections in Fig. 5, the energy scale has been shifted by the appropriate barrier height.³ Figure 5 indicates that the one-neutron transfer for $^{58}\text{Ni} + ^{64}\text{Ni}$, which has the larger fusion cross section, is about an order of magnitude larger than that of $^{64}\text{Ni} + ^{64}\text{Ni}$ at far sub-barrier energies.

Geometrical effects can be approximately removed by dividing the cross sections by the square of the appropriate radius parameters appearing in Table III. The resulting geometrically renormalized fusion cross sections for $^{58}\text{Ni} + ^{58}\text{Ni}$ and $^{64}\text{Ni} + ^{64}\text{Ni}$ are almost identical³ while, at bombarding energies 5% below barrier, the renormalized fusion of $^{58}\text{Ni} + ^{64}\text{Ni}$ is about 50 times larger than that resulting from symmetric projectile-target combinations. Transfer would be expected to be relatively unimportant for the symmetric reactions because of the significantly more negative Q values for neutron and neutron pair transfers. The Q values for ground state transfers along with the optimum Q values using the prescription of Alder *et al.*¹⁸ are presented in Table III.

TABLE III. Summary of Q values (MeV) and interaction barrier systematics for Ni-Ni reactions.

	$^{58}\text{Ni} + ^{64}\text{Ni}$	$^{64}\text{Ni} + ^{64}\text{Ni}$	$^{58}\text{Ni} + ^{58}\text{Ni}$
Q (1n) pickup	-0.66	-3.56	-3.22
Q_{opt}^a	0.26	0.32	0.39
Q (2n) pickup	+3.89	-1.43	-2.08
Q_{opt}^b	0.50	0.62	0.75
Q (2p) stripping	+2.18	-6.44	-5.66
Q_{opt}^b	-0.46	-0.43	-0.43
V_0 (MeV) ^c	96.0	93.5	97.9
R_0 (fm)	8.2	8.6	8.3
r_0 (fm)	1.04	1.08	1.07
$\hbar\omega$ (MeV)	4.0	4.0	4.0

^aOptimum Q values are evaluated at 170 MeV bombarding energy for 180° scattering using the prescription in Ref. 18.

^bOptimum Q value for pair transfers are evaluated assuming a one-step process using the expressions given in Ref. 18.

^cInverted harmonic oscillator potential parameters taken from Ref. 3.

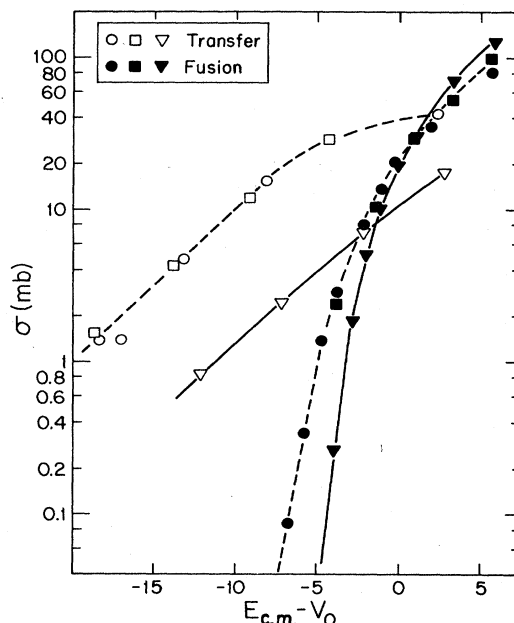


FIG. 5. Excitation functions with abscissa as the center of mass energy relative to the appropriate barrier height V_0 (Table III). Symbols correspond to the same beam-target combinations as in Fig. 3: $^{58}\text{Ni} + ^{64}\text{Ni}$ (circles), $^{64}\text{Ni} + ^{58}\text{Ni}$ (squares), and $^{64}\text{Ni} + ^{64}\text{Ni}$ (triangles). Open symbols represent one-neutron transfer leading to the 155.5 keV state of ^{63}Ni , and total one-neutron transfer is estimated to be between 20% and 50% larger than this cross section. The filled symbols represent the corresponding fusion data. The transfer data from $^{64}\text{Ni} + ^{64}\text{Ni}$ include both pickup and stripping processes.

Of equal importance to the observation that the sub-barrier one-neutron transfer cross section for $^{58}\text{Ni} + ^{64}\text{Ni}$ is almost an order of magnitude larger than that of $^{64}\text{Ni} + ^{64}\text{Ni}$, is the fact that the sub-barrier transfer cross sections are much larger than those of fusion. One-nucleon transfer may be an important mechanism in understanding the isotopic dependence of sub-barrier fusion from Ni-Ni interactions.

V. CONCLUSIONS

The measurement of transfer-characteristic γ rays is shown to be a successful method of determining sub-barrier transfer cross sections to excited states. Our analysis shows that the first-order DWBA correctly describes the one-neutron transfer excitation functions at sub-barrier energies between heavy, symmetric nuclei. For $^{58}\text{Ni} + ^{64}\text{Ni}$, one-neutron transfer is near Q_{opt} and the cross sections for this reaction are well described over the measured bombarding energy range. The one-neutron transfer from $^{64}\text{Ni} + ^{64}\text{Ni}$ has lower cross section and is not well Q matched. The DWBA calculations of this reaction underpredict the one-neutron transfer cross sections near the barrier but still provide a good description

of the data at energies lower than 7% below the barrier. The calculations of Coulomb excitation discussed in Sec. II A demonstrate that, for $E_{c.m.} < 90$ MeV, the target and projectile are both in their ground states at the distance of closest approach with at least a 90% probability.

The spectroscopic factors (presented in Tables I and II) connecting the observed transfer product excited states and the ground states of the target and projectile are all large, implying that the spectroscopic factors connecting these particular states to the 2_1^+ states, of either the target or projectile, are small. The cross section for multiple Coulomb excitation is small and none of the transfer product states with small (ground state) spectroscopic factors are observed. The close agreement of the calculations with the data, along with these considerations, lead to the conclusion that these sub-barrier one-neutron transfer cross sections are dominated by the one-step mechanism from the ground states of the target and projectile.

One-nucleon transfer cross sections can be larger than 1 mb at bombarding energies 20% below the barrier, and the importance of the nucleon transfer channel at sub-

barrier energies cannot be overlooked. At a bombarding energy where the sub-barrier fusion of $^{58}\text{Ni} + ^{64}\text{Ni}$ is about 50 times larger than that of $^{64}\text{Ni} + ^{64}\text{Ni}$, the one-neutron transfer for $^{58}\text{Ni} + ^{64}\text{Ni}$ is about a factor of 40 larger than the $^{58}\text{Ni} + ^{64}\text{Ni}$ fusion. Therefore, even without considering other reaction channels such as nucleon pair transfer, there is sufficient one-nucleon transfer below the barrier which may significantly influence fusion.

ACKNOWLEDGMENTS

We sincerely thank Dr. Pollarolo for supplying parentage coefficients for the ground and excited states of the even nickel isotopes prior to publication. We thank the members of the operations staff of the Brookhaven National Laboratory Tandem Van de Graaff Facility for their hospitality and assistance. This work was supported primarily by the U.S. Department of Energy under Contract No. AC02-76ER03069. F.V. and S.G.S. acknowledge the support of the Danish National Science Research Council.

*Present address: Nuclear Science Division, Lawrence Berkeley Laboratory, Berkeley, CA 94720.

¹J. R. Oppenheimer and M. Phillips, *Phys. Rev.* **18**, 500 (1935).

²G. Breit, M. H. Hull, Jr., and A. L. Gluckstern, *Phys. Rev.* **87**, 74 (1952).

³M. Beckerman, J. Ball, H. Enge, M. Salomaa, A. Sperduto, S. Gazes, A. DiRienzo, and J. D. Molitoris, *Phys. Rev. C* **23**, 1581 (1981); M. Beckerman, M. Salomaa, A. Sperduto, J. D. Molitoris, and A. DiRienzo, *ibid.* **25**, 837 (1982).

⁴A. B. Balantekin, S. E. Koonin, and J. W. Negele, *Phys. Rev. C* **28**, 1565 (1983).

⁵R. A. Broglia, C. H. Dasso, S. Landowne, and A. Winther, *Phys. Rev. C* **27**, 2433 (1983).

⁶C. H. Dasso, S. Landowne, and A. Winther, *Nucl. Phys.* **A405**, 381 (1983); S. Landowne and S. C. Pieper, *Phys. Rev. C* **29**, 1352 (1984); M. J. Rhoades-Brown and P. Braun-Munzinger, *Phys. Lett.* **136B**, 19 (1984).

⁷K. Alder, A. Bohr, T. Huus, B. Mottleson, and A. Winther, *Rev. Mod. Phys.* **28**, 432 (1956).

⁸P. R. Christensen, S. Pontoppidan, F. Videbaek, J. Barrette, P. D. Bond, Ole Hansen, and C. E. Thorn, *Phys. Rev. C* **29**, 455 (1984).

⁹S. Cohen, R. D. Lawson, M. H. Macfarlane, S. P. Pandya, and M. Soga, *Phys. Rev.* **160**, 903 (1967).

¹⁰R. A. Broglia and A. Winther, *Phys. Rep.* **4**, 153 (1972); R. A. Broglia, R. Liotta, B. S. Nilsson, and A. Winther, *ibid.* **29**, 291 (1977); B. S. Nilsson (unpublished).

¹¹P. R. Christensen and A. Winther, *Phys. Lett.* **65B**, 19 (1976).

¹²R. H. Fulmer and A. L. McCarthy, *Phys. Rev.* **131**, 2133 (1963); R. H. Fulmer, A. L. McCarthy, R. L. Cohen, and R.

Middleton, *ibid.* **133**, B955 (1964); E. R. Cosman, C. H. Paris, A. Sperduto, and H. Enge, *ibid.* **142**, 673 (1966); I. M. Turkiewicz, P. Beuzit, J. Delanay, and J. P. Fouan, *Nucl. Phys.* **A143**, 641 (1970); V. F. Litvin, Yu. A. Nemilov, L. V. Krasnov, K. A. Gridnev, K. I. Zhrebztzova, Yu. A. Lakomkin, T. V. Orlova, V. P. Bochin, and V. S. Romanov, *ibid.* **A184**, 105 (1972); P. Staub, E. Baumgartner, J. X. Saladin, H. Schar, and D. Trautmann, *Helv. Phys. Acta* **50**, 9 (1977); E. R. Flynn, R. E. Brown, F. D. Correll, D. L. Hanson, and R. A. Hardekopf, *Phys. Rev. Lett.* **42**, 626 (1979); T. Taylor and J. A. Cameron, *Nucl. Phys.* **A337**, 389 (1980).

¹³R. H. Fulmer and W. W. Daehnick, *Phys. Rev.* **139**, B579 (1965).

¹⁴P. D. Bond, O. Hansen, C. E. Thorn, M. J. LeVine, P. R. Christensen, S. Pontoppidan, F. Videbaek, J. Cheng-Lie, and M. M. Rhoades-Brown, *Phys. Lett.* **114B**, 423 (1982).

¹⁵R. L. Auble, *Nucl. Data Sheets* **14**, 119 (1975).

¹⁶N. Pollarolo (private communication).

¹⁷See, e.g., L. J. B. Goldfarb and W. von Oertzen, in *Heavy Ion Collisions*, edited by R. Boch (North-Holland, Amsterdam, 1979), Vol. I, p. 217; H. G. Bohlen, W. von Oertzen, W. Bohme, and B. Gebauer, *Phys. Rev. Lett.* **37**, 195 (1976); B. F. Bayman and Jongsheng Chen, *Phys. Rev. C* **26**, 1509 (1982); M. A. Franey, B. F. Bayman, J. S. Lilley, and W. R. Phillips, *Phys. Rev. Lett.* **41**, 837 (1978); U. Gotz, M. Ichimura, R. A. Broglia, and A. Winther, *Phys. Rep.* **16C**, 115 (1975); M. A. Franey, J. S. Lilley, and W. R. Phillips, *Nucl. Phys.* **A324**, 193 (1979).

¹⁸K. Alder, R. Morf, M. Pauli, and D. Trautmann, *Nucl. Phys.* **A191**, 399 (1972).